



## Estimated changes in different forms of precipitation (snow, sleet, and rain) across China: 1961–2016

Bo Su<sup>a,b</sup>, Cunde Xiao<sup>a</sup>, Hongyu Zhao<sup>a</sup>, Yi Huang<sup>a</sup>, Tingfeng Dou<sup>c</sup>, Xuejia Wang<sup>d</sup>, Deliang Chen<sup>b,\*</sup>

<sup>a</sup> State Key Laboratory of Earth Surface Processes and Resource Ecology, Beijing Normal University, Beijing 100875, China

<sup>b</sup> Regional Climate Group, Department of Earth Sciences, University of Gothenburg, Box 460, 405 30 Gothenburg, Sweden

<sup>c</sup> College of Resources and Environment, University of Chinese Academy of Sciences, Beijing 100049, China

<sup>d</sup> Key Laboratory of Western China's Environmental Systems (Ministry of Education), College of Earth and Environmental Sciences, Lanzhou University, Lanzhou 730030, China

### ARTICLE INFO

#### Keywords:

Precipitation phase  
Temperature thresholds  
Wet-bulb temperature  
Climatology  
Trend  
China

### ABSTRACT

Different forms of precipitation (snow, sleet, and rain) have divergent effects on the Earth's surface water and energy fluxes. Therefore, discriminating between these forms, and exploring their climatology and variations are of significant importance, especially under a changing climate. In this study, a state-of-the-art parameterization scheme with wet-bulb temperature ( $T_w$ ), relative humidity ( $RH$ ), surface air pressure, and elevation as inputs was used to estimate the climatologies and trends of the different forms of precipitation and their temperature thresholds across China mainland from 1961 to 2016. The results indicate that on average, only 9.6% and 0.8% of the total precipitation (602.9 mm) over China during 1961–2016 occurred as snow and sleet. The trends of the different forms of precipitation varied greatly from region to region and from season to season. The regionally averaged annual precipitation, rainfall, and snowfall across China significantly increased at rates of 11.4 mm/decade, 11.0 mm/decade, and 1.0 mm/decade, respectively, whereas the annual sleet decreased at a rate of  $-0.3$  mm/decade. The region-wide snow (rain) fraction significantly increased (decreased) in Northwestern China (NWC) and Northern China (NC) but significantly decreased (increased) on the Tibetan Plateau (TP). Given the heterogeneous  $RH$  and complex topography, the  $T_w$  values at which snow-sleet and sleet-rain occurred with equal frequency—that is,  $T_s$  and  $T_r$ , varied significantly across China, averaging  $0.1$  °C and  $0.3$  °C, respectively. However, most regions experienced significant decreases in the temperature thresholds (especially  $T_r$ ), with decreasing  $RH$ . Almost all of the regions also experienced significant increases in  $T_w$ , especially on the TP and during the winter and spring. The adverse combination of the increase in  $T_w$  and the decrease in the temperature thresholds resulted in more precipitation falling as rain, although the snowfall slightly increased in some regions.

### 1. Introduction

Different forms of precipitation (snow, sleet, and rain) have divergent effects on the water and energy fluxes of the Earth (Jennings et al., 2018; Loth et al., 1993; Marks et al., 1992). The presence of snow is beneficial to the formation and development of terrestrial and marine cryosphere components such as glaciers, frozen ground, snow cover, and sea ice by increasing the surface albedo and through mass accumulation. On the contrary, rainfall accelerates cryosphere shrinkage through changes in the surface energy budget such as the reduction in the surface

albedo and the release of latent heat (Ding et al., 2014; Ding et al., 2017; Dou et al., 2021; Flanner et al., 2011; Su et al., 2022). Sleet plays a more complex role in cryosphere changes and is relatively challenging to classify. As the global air temperature continues to increase, the resultant changes in different types of precipitation exert profound impacts on the cryosphere's components, with widespread meteorological, hydrological, ecological, and socioeconomic consequences (e.g., Ma et al., 2020; Mankin and Duffenbaugh, 2015; Musselman et al., 2021; You et al., 2020; Zhong et al., 2018). This is especially true for extensive cold and arid regions of the world. Therefore, discriminating between

\* Corresponding author.

E-mail address: [deliang@gvc.gu.se](mailto:deliang@gvc.gu.se) (D. Chen).

<https://doi.org/10.1016/j.atmosres.2022.106078>

Received 14 October 2021; Received in revised form 6 February 2022; Accepted 7 February 2022

Available online 10 February 2022

0169-8095/© 2022 The Authors. Published by Elsevier B.V. This is an open access article under the CC BY license (<http://creativecommons.org/licenses/by/4.0/>).

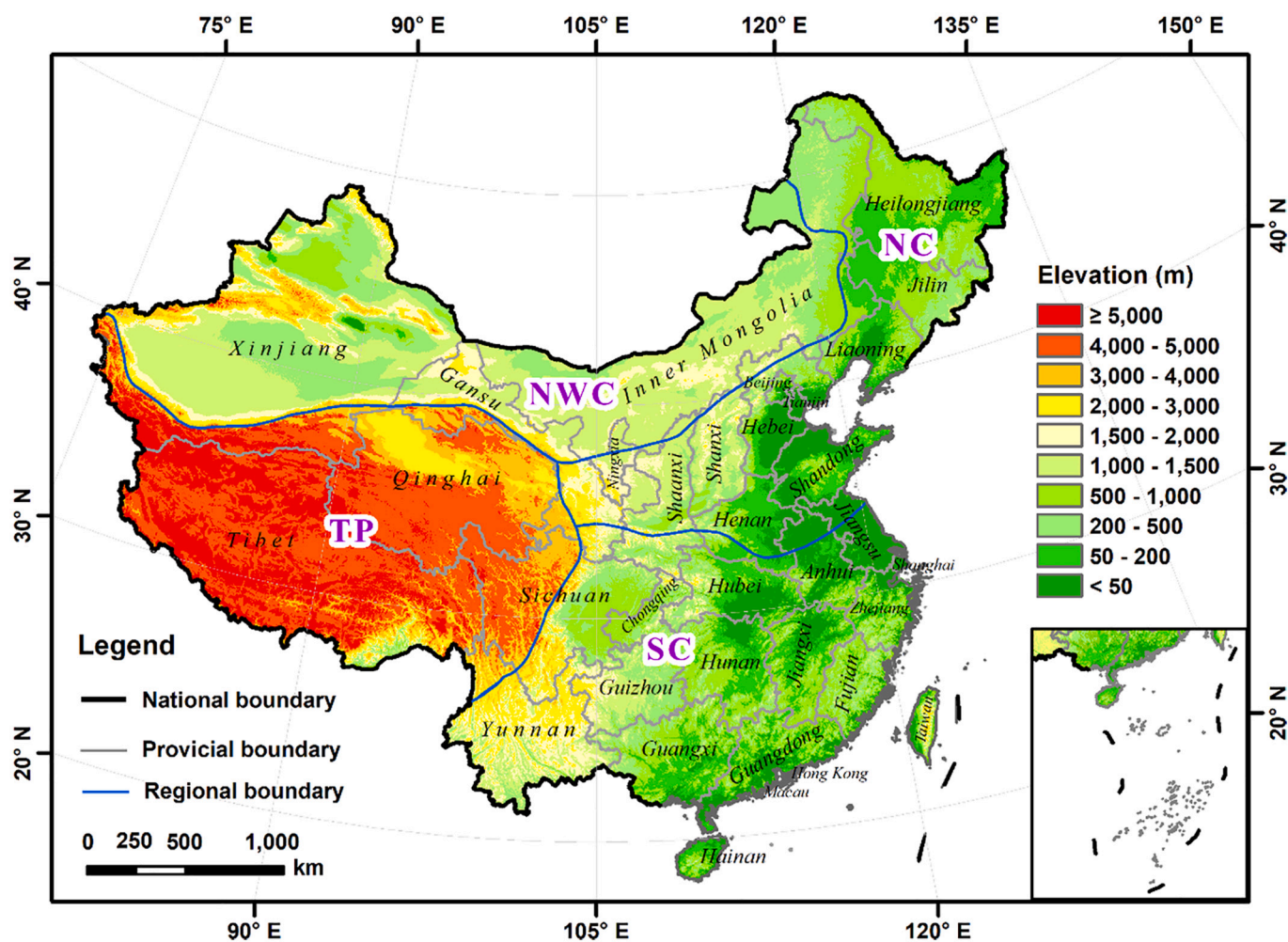


Fig. 1. Geological map of China showing location, elevation, and regionalization. The country was divided into four sub-regions according to the geographic regionalization of China, i.e., Northwestern China (NWC), Northern China (NC), Tibetan Plateau (TP), and Southern China (SC) (Zhao 1995).

precipitation types and exploring their changes are of significant importance and have received increasing attention (Jennings et al., 2018; Knowles et al., 2006; Li et al., 2020; Serquet et al., 2011).

Continuous observations of precipitation types can provide accurate information for a deep understanding of the climatology, variations, and impacts of different forms of precipitation. Such data are also vital input variables for cryospheric, hydrologic, and climate models (Ding et al., 2014; Jennings et al., 2018; You et al., 2020). However, the observed precipitation types are often limited or not accessible, which is especially true in the alpine and polar regions, where snowfall is concentrated and weather stations are sparse. In this case, the discrimination between the precipitation types wildly relies on empirical schemes, in which temperature thresholds play an especially important role and are used to assign different forms of precipitation. The thresholds are generally derived from vertical profiles of air temperature and other atmospheric conditions or the relationships between the existing observed precipitation types and the other meteorological variables such as the air temperature, wet-bulb temperature ( $T_w$ ), relative humidity ( $RH$ ), and surface elevation (Ding et al., 2014). The temperature thresholds for discriminating between precipitation types are also highly temporally and spatially heterogeneous because they are highly dependent on the local atmospheric and geographical conditions (Ye et al., 2013; Jennings et al., 2018).

Numerous studies have investigated the changes in the different types of precipitation during the last few decades. These studies have generally concluded that global-scale precipitation has likely increased

since the mid-20th century. Furthermore, there has been a shift from snowfall to rainfall, and the shift are projected to continue through this century (Krasting et al., 2013; Berghuijs and Woods, 2014; IPCC, 2021). Due to pronounced climate change, the snowfall fraction, i.e., the proportion of precipitation occurring as snowfall, has significantly decreased in many regions of the world (Krasting et al., 2013; Räisänen, 2008), such as in New England (Huntington et al., 2004), United States (Knowles et al., 2006; Song and Qi, 2007), Switzerland (Serquet et al., 2011), Finland (Irannezhad et al., 2017), the Tibetan Plateau (TP hereafter) (Deng et al., 2017; Wang et al., 2016; Li et al., 2022), the alpine regions of Central Asia (Guo and Li, 2015; Li et al., 2020; Yang et al., 2020), and even the Arctic and Antarctic regions (Dou et al., 2021; Han et al., 2018; Yang et al., 2021). In contrast, the rainfall fraction, i.e., the proportion of precipitation occurring as rain, has increased overall (Dou et al., 2021; Knowles et al., 2006). Spatially uniform temperature thresholds are commonly used in many land surface models although the importance of the precipitation type. However, Jennings et al. (2018) created the first Northern Hemisphere rain-snow threshold map through the analysis of observational datasets, and their results indicate that the air temperature at which the occurrence probabilities of rain and snow are equal to each other varies from  $-0.4$  to  $2.4$  °C, averaging  $1.0$  °C for 95% of the stations.

For China, the data on the precipitation types for more than 700 weather stations from the 1950s to 1979 can be obtained from the National Meteorological Information Center (NMIC) of the China Meteorological Administration (CMA), but data are not available for the years

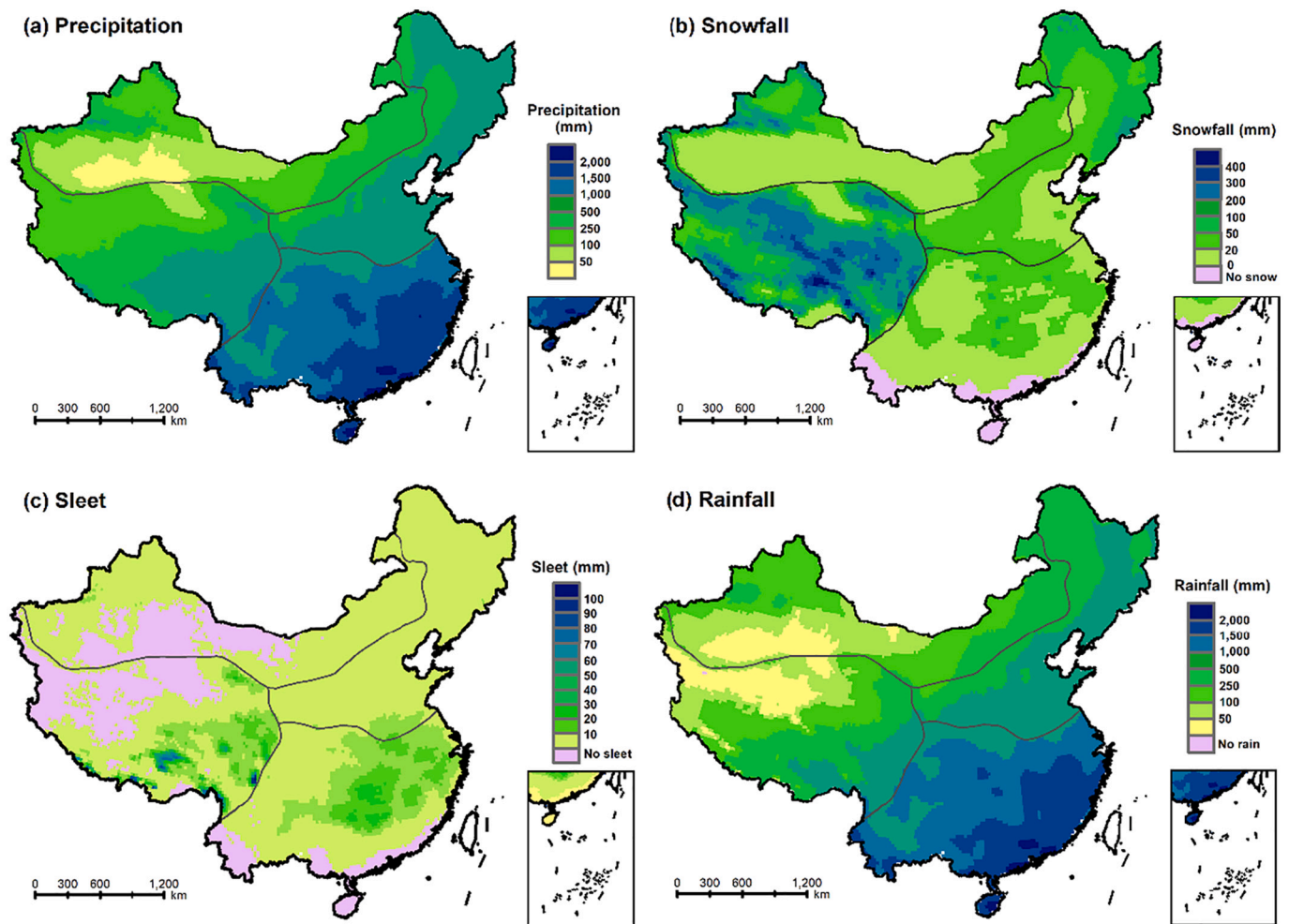


Fig. 2. Climatologies of the different forms of precipitation during 1961–2016: (a) total amount of precipitation, (b) snowfall, (b) sleet, and (d) rainfall.

after 1979 (Ding et al., 2014). Based on more than 400,000 samples for which the precipitation types are available across China, a state-of-the-art parameterization scheme based on  $T_w$ ,  $RH$ , surface pressure, and elevation information was developed by Ding et al. (2014) to discriminate between precipitation types. Many studies have also explored the site-based changes in snowfall and/or its fraction in China (Liu et al., 2012; Zhang et al., 2016a), with a focus on the TP (Deng et al., 2017), northern Xinjiang, including the Tianshan Mountains (Wang et al., 2017a,b; Li et al., 2020; Yang et al., 2020), and Northeastern China (Zhao et al., 2009; Hou et al., 2019; Jiang and Sun, 2019) (i.e., the three main snowfall regions of China) using the scheme proposed by Ding et al. (2014), or other methods such as air temperature-based thresholds, temperature profiles, or limited observation data. These studies have demonstrated that the spatial and seasonal variations in snowfall and its fraction are large in China. Nevertheless, to date, no comprehensive climatology and trends of the different types of precipitation (snow, sleet, and rain) have been presented. For the alpine and TP regions, especially across western China, the understanding of the changes in the different types of precipitation still needs to be strengthened because the weather stations are indeed sparse (You et al., 2020). In addition, the spatiotemporal patterns of the snow-sleet and sleet-rain thresholds remain to be explored under a changing climate to enable comprehensive cause analysis of the changes in the different types of precipitation.

To address these gaps, we systematically investigated the climatology and trends of the different types of precipitation (snow, sleet, and rain) and their thresholds and the associated  $T_w$  and  $RH$  in China during 1961–2016 in this study, by applying the state-of-the-art

parameterization scheme and observational gridded datasets, with a maximum spatial resolution of  $0.25^\circ$ . The knowledge and dataset released in this study may benefit various research communities, such as cryosphere science, hydrology, ecology, and climate change, and the results provide a scientific basis for decision-making for regional sustainable development.

## 2. Study area, data, and methods

### 2.1. Study area

China is located in the eastern part of the Eurasian Continent ( $73^\circ 4' - 135^\circ 2' E$ ,  $53^\circ 33' N - 3^\circ 52' S$ ). In this study, we further divided the country into four sub-regions according to the geographic regionalization of China, i.e., Northwestern China (NWC), Northern China (NC), the TP, and Southern China (SC) (Ma et al., 2020; Zhao, 2005) (Fig. 1). The TP has a mean elevation of  $\sim 4000$  m above sea level, and it is known as the Third Pole of the Earth and the Water Tower of Asia (Yao et al., 2012; Zhang et al., 2020). Both NC and SC are dominated by the Asian monsoon, but they are approximately separated by the 800 mm annual isohyet and by the  $0^\circ C$  isotherm line in January (Zhao, 2005). In addition, the climate in NWC is continental, with annual precipitation of less than 400 mm because it is situated in the interior of the Eurasian hinterland and is far from any ocean (Chen et al., 2016).

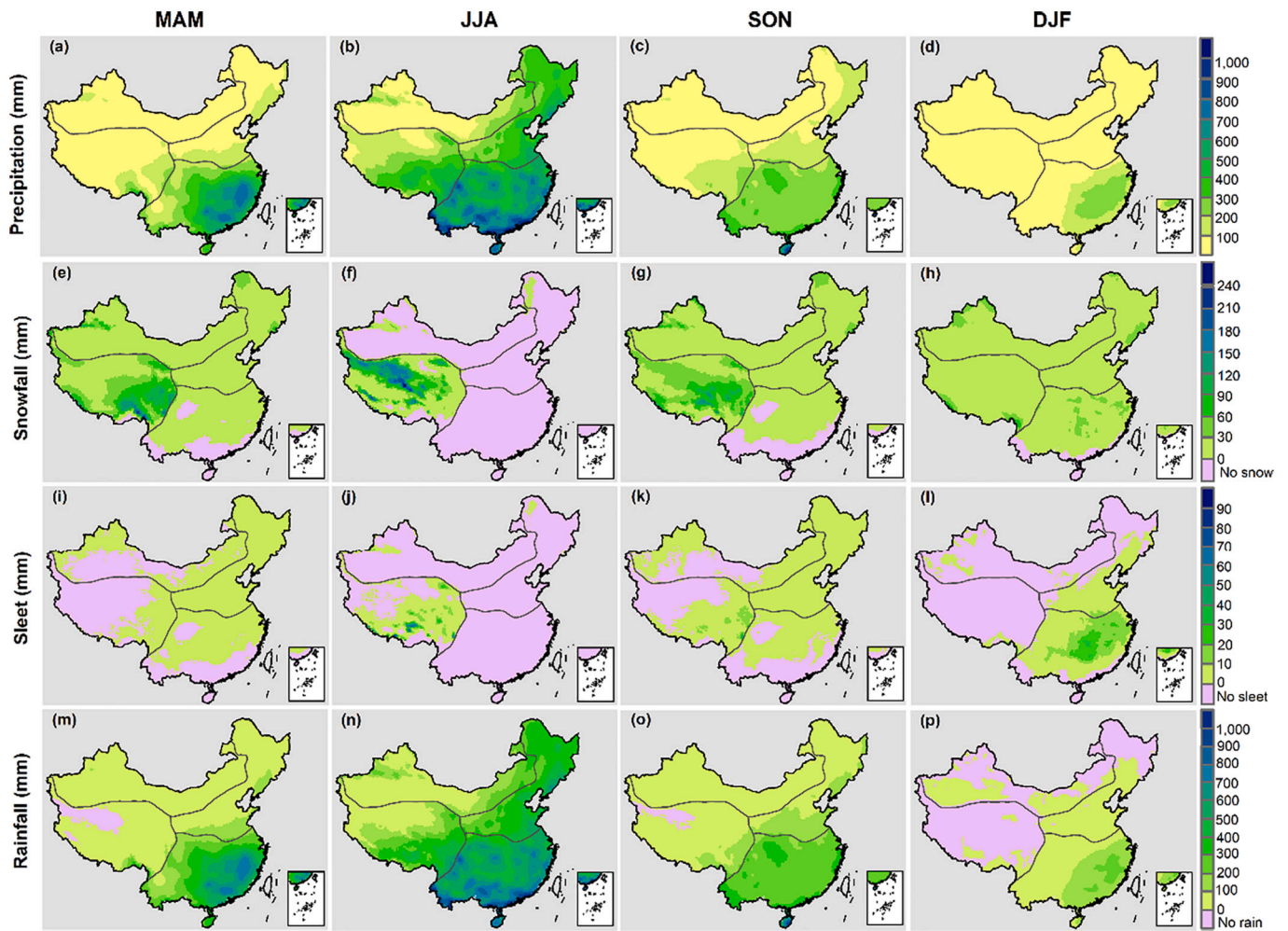


Fig. 3. Spatial distribution of the seasonal climatologies of the different forms of precipitation over China during 1961–2016. (a–d) total amount of precipitation, (e–h) snowfall, (i–l) sleet, and (m–p) rainfall. Note: Spring (March–May, MAM), Summer (June–August, JJA), Autumn (September–November, SON), and Winter (December–February, DJF).

## 2.2. Data sources

To discriminate between the precipitation types, daily weather data (including air temperature, precipitation,  $RH$ , and surface pressure) and elevation data were employed in this study. Among them, the daily air temperature, precipitation, and  $RH$  data were obtained from an observational gridded dataset CN05.1 with a spatial resolution of  $0.25^\circ$  (Wu and Gao, 2013), which was developed by the Climate Change Research Center, Chinese Academy of Sciences (<http://ccrc.iap.ac.cn/>). The CN05.1 was interpolated based on 2416 stations in China (Wu and Gao, 2013) and has been widely used in the assessment and validation of climate change on national and subnational scales (e.g., Guo et al., 2018; Wang et al., 2020). The daily surface pressure was obtained from the NCEP/NCAR Reanalysis 1 dataset with a spatial resolution of  $2.5^\circ \times 2.5^\circ$ , (available at <https://psl.noaa.gov/data/gridded/data.ncep.reanalysis.surface.html>). The elevation data (SRTMDEM) with a spatial resolution of 90 m were obtained from the Geospatial Data Cloud site, Computer Network Information Center, Chinese Academy of Sciences (<http://www.gscloud.cn>). Due to the different spatial resolutions, we further interpolated the surface pressure and elevation datasets to a common resolution of  $0.25^\circ \times 0.25^\circ$ . In addition, the administrative boundary data were obtained from the Data Center for Resources and Environmental Sciences (DCRES), Chinese Academy of Sciences (CAS) (<http://www.resdc.cn>).

## 2.3. Methods

### 2.3.1. Discrimination of precipitation type

We employed the parameterization scheme proposed by Ding et al. (2014) to discriminate between the precipitation types and to calculate the different forms of precipitation (Eqs. 1–8).

$$P_{\text{type}} = \begin{cases} \text{snow, if } T_w \leq T_s \\ \text{sleet, if } T_s \leq T_w \leq T_r \\ \text{rain, if } T_w \geq T_r \end{cases} \quad (1)$$

where  $P_{\text{type}}$  is the daily precipitation types, i.e., snow, sleet, and rain; and  $T_s$  and  $T_r$  are the snow-sleet and sleet-rain threshold temperatures [ $^\circ\text{C}$ ], respectively.  $T_w$  can be calculated as follows:

$$T_w = T_a - \frac{e_{\text{sat}}(T_a) \times (1 - RH)}{0.000643 \times P_s + \frac{\partial e_{\text{sat}}}{\partial T}} \quad (2)$$

In Eq. (2),  $T_a$  is the daily temperature [ $^\circ\text{C}$ ]; and  $e_{\text{sat}}(T_a)$  is the saturated vapor pressure [hPa] at  $T_a$  and is given by Tetens's empirical formula (Murray, 1967):

$$e_{\text{sat}}(T_a) = 6.1078 \times e^{\left(\frac{17.27 \times T_a}{T_a + 237.3}\right)}. \quad (3)$$

$T_r$  is the temperature value at which rain and sleet fall with equal frequency, and  $T_s$  is that for the equal occurrence frequency of snow and

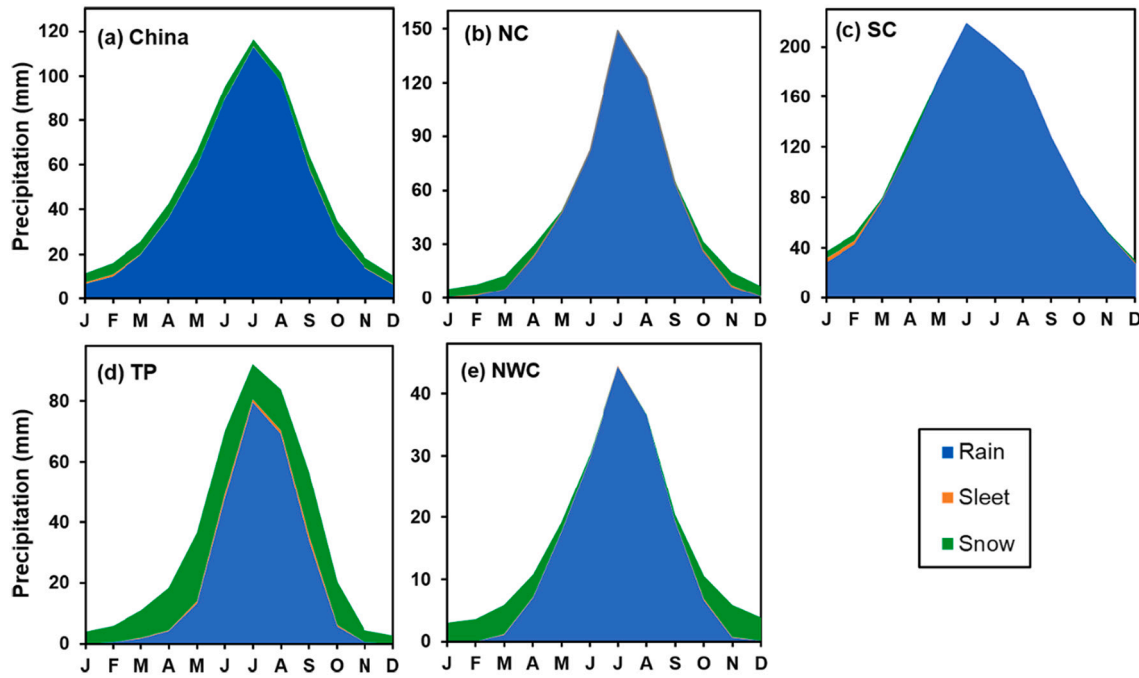


**Fig. 4.** Annual climatological cycles of the different forms of precipitation during 1961–2016 (a) over China and in the four sub-regions: (b) Northern China (NC), (c) Southern China (SC), (d) Tibetan Plateau (TP), and (e) Northwestern China (NWC). The values in horizontal axis represent the months from January to December.

sleet. The two threshold temperatures are as follows:

$$T_s = \begin{cases} T_0 - \Delta S \times \ln \left[ e^{\left( \frac{\Delta T}{\Delta S} \right)} - 2e^{\left( -\frac{\Delta T}{\Delta S} \right)} \right], & \text{if } \frac{\Delta T}{\Delta S} > \ln 2 \\ T_0, & \text{if } \frac{\Delta T}{\Delta S} \leq \ln 2 \end{cases} \quad (4)$$

$$T_r = \begin{cases} 2 \times T_0 - T_s, & \text{if } \frac{\Delta T}{\Delta S} > \ln 2 \\ T_0, & \text{if } \frac{\Delta T}{\Delta S} \leq \ln 2 \end{cases} \quad (5)$$

In Eqs. (4–5),  $T_0$  depends on both the elevation ( $Z$ ) [m.a.s.l.] and  $RH$  [%] and is calculated as follows:

$$T_0 = -5.87 - 0.1042 \times Z + 0.0885 \times Z^2 + 16.06 \times RH - 9.614 \times RH^2 \quad (6)$$

$\Delta T$  and  $\Delta S$  are the temperature difference and temperature scale, respectively, and can be calculated as follows:

$$\Delta T = 0.215 - 0.099 \times RH + 1.018 \times RH^2 \quad (7)$$

$$\Delta S = 2.374 - 1.634 \times RH \quad (8)$$

### 2.3.2. Statistic analysis

To detect the trends of the different forms of precipitation (rain, sleet, and snow), their temperature thresholds, and the associated  $T_w$  and  $RH$  values, Sen’s slope was used to estimate the slopes of the trends (Sen, 1968), and the nonparametric Mann–Kendall trend test was applied to quantify the significance of the trends at a confidence level of 95% ( $p < 0.05$ ) (Mann, 1945; Kendall, 1948).

## 3. Results

### 3.1. Climatologies of the different forms of precipitation

The long-term (1961–2016) mean annual precipitation exhibited an overall decreasing trend from southeast to northwest across China (Ding, 2013), averaging 602.9 mm and ranging from 22.8 mm to 2300.5

mm (Fig. 2(a)). Among them, rainfall accounted for the vast majority of the precipitation (89.5%), and the overall climatology was almost consistent with that of the precipitation spatially (Fig. 2(d)). Nearly 9.6% and 0.8% of the precipitation occurred as snow and sleet, respectively. The snowfall was mainly concentrated on the TP and in northern Xinjiang, including the Tianshan Mountains and northeastern China (mainly in the Greater and Lesser Khingan Ranges, and the Changbai Mountains) (Fig. 2(b)) (Liu et al., 2012; Zhang et al., 2016a; Zhang et al., 2016b). The sleet had high values on the southeastern TP and in the middle and lower reaches of the Yangtze River Basin (Fig. 2(c)). The southernmost areas of the SC were considered to be snow-free and sleet-free regions because snowfall and sleet events were scarce in these areas. The arid areas of the interior of the TP and NWC were also mainly sleet-free regions. On a regional scale, the mean annual precipitation was largest in SC (1363.2 mm), in which 97.8% (1333.1 mm) of the precipitation occurred as rain, and only ~1.7% (20.6 mm) and ~0.7% (9.5 mm) occurred as snow and sleet, respectively. The mean annual precipitation in NWC was 194.0 mm, and the mean proportions of snowfall, sleet, and rainfall were 15.6%, 0.4%, and 84.0%, respectively. The snowfall accounted for the highest proportion of the mean annual precipitation (405.7 mm) on the TP, reaching 35.0% with a mean annual snowfall of 142.0 mm. The mean annual snowfall was higher (41.5 mm) in NC, but its proportion of the mean total precipitation was relatively low (only 7.2%) due to the higher mean annual rainfall (531.7 mm) in this region.

Fig. 3 illustrates the average spatial distributions of the seasonal climatologies of the different forms of precipitation during 1961–2016. The climatological annual cycles are shown in Fig. 4. Overall, the regional mean precipitation and rainfall were concentrated from May to September in China as a whole and in the four sub-regions. However, the snowfall and sleet were concentrated from October to April in NC, SC, and NWC, in which the mean snowfall during this season accounted for 97.5%, 99.7%, and 90.3% of the mean annual snowfall, respectively. However, in SC, the winter snowfall accounted for only 11.1% of the total precipitation. Differing from the other regions, the mean snowfall across the TP was large in spring (45.7 mm) and summer (45.5 mm), followed by autumn (39.0 mm), and it was smallest in winter (11.8 mm)

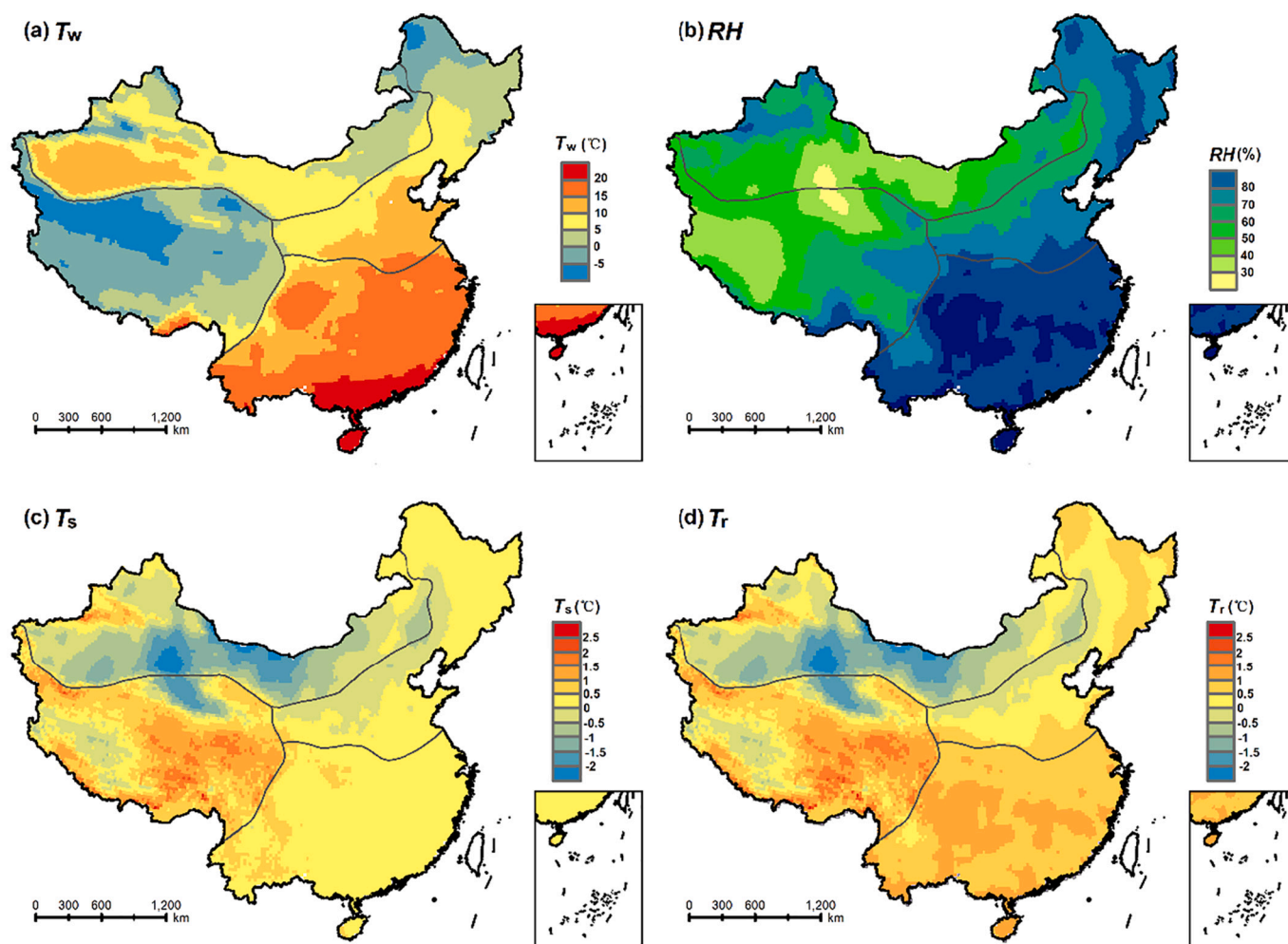


Fig. 5. Climatology of (a) wet-bulb temperature ( $T_w$ ), (b) relative humidity ( $RH$ ), and the  $T_w$  values at which snow-sleet and sleet-rain occurred with equal frequency—that is, (c)  $T_s$  and (d)  $T_r$  during 1961–2016.

due to the overall lower amount of precipitation in this season. Moreover, the mean sleet on the TP was concentrated from May to September (85.0% of 5.9 mm).

### 3.2. Climatologies of temperature thresholds ( $T_s$ and $T_r$ ) and associated $T_w$ and $RH$

The climatologies of the different forms of precipitation (snow, sleet, and rain) were determined based on not only the pattern of the total precipitation but also on their temperature thresholds and associated factors, including the  $RH$  and land surface elevation. As can be seen from Fig. 1, the elevation of China decreases in a three-step staircase pattern from west to east (Deng et al., 2020; Zhao, 2005). The first step is the TP, where the average elevation is above 4000 m. The second step mainly includes the Inner Mongolia Plateau, the Loess Plateau, the Yunnan-Guizhou Plateau, and several basins such as the Tarim, Junggar, and Sichuan basins, with average elevations of 1500–2500 m. The third step primarily consists of the plains and hills in eastern and southern China, where the elevations are mostly less than 500 m. The climatology of the  $RH$  was generally consistent with that of the total precipitation across China (Fig. 5(b)).

Given the heterogeneous  $RH$  and complex topography, the  $T_w$  at which snow and sleet (rain and sleet) occur with equal frequency, i.e.,  $T_s$  ( $T_r$ ), varied significantly across China (Figs. 5(c–d)). High altitude and humid areas generally exhibited warmer thresholds (both  $T_s$  and  $T_r$ ), while low altitude and arid areas exhibited colder thresholds. The

annual mean  $T_s$  ( $T_r$ ) was 0.1 °C (0.3 °C) in China, ranging from  $-2.3$  °C to 2.8 °C ( $-2.3$  °C to 2.9 °C), with the highest  $T_s$  and  $T_r$  values occurring on the southeastern TP and lowest values occurring in the desert areas of NWC. The climatology of the  $T_s$  also coincided with that of  $T_r$  in the TP and NWC regions; but the difference between the  $T_s$  and  $T_r$  values were larger in SC and NC due to the large  $RH$  values, indicating a larger proportion of the precipitation occurred as sleet in these regions. The annual mean  $T_s$  ( $T_r$ ) in NC, SC, NWC, and TP were 0.1 °C (0.3 °C), 0.4 °C (0.9 °C),  $-0.6$  °C ( $-0.5$  °C), and 0.6 °C (0.6 °C), respectively. The spatial distributions of the seasonal mean  $T_s$  and  $T_r$  also varied from season to season (Figs. 6(i–p)) due to the seasonal variations in  $RH$  (Figs. 6(e–h)).

The climatology of  $T_w$  exhibited an understandable latitudinal zonal pattern in eastern China, and a significant elevation dependence in western China on both annual (Fig. 5(a)) and seasonal (Figs. 6(a–d)) scales, which is also generally consistent with the patterns of the air temperature (Ding, 2013; Zhao, 2005). The climatology of  $T_w$  determines the proportions of the different forms of precipitation and the spatial patterns of the  $T_w$  thresholds ( $T_s$  and  $T_r$ ).

### 3.3. Changes in the different forms of precipitation

From 1961 to 2016, approximately 72.7% of the land area exhibited an increase in the annual precipitation, and the significant increasing trends (23.5% of the land area) mainly occurred in northern Xinjiang (including the Tianshan Mountains) and northeastern Tibet. In contrast, decreasing trends were mainly detected in the southern NC, western SC,

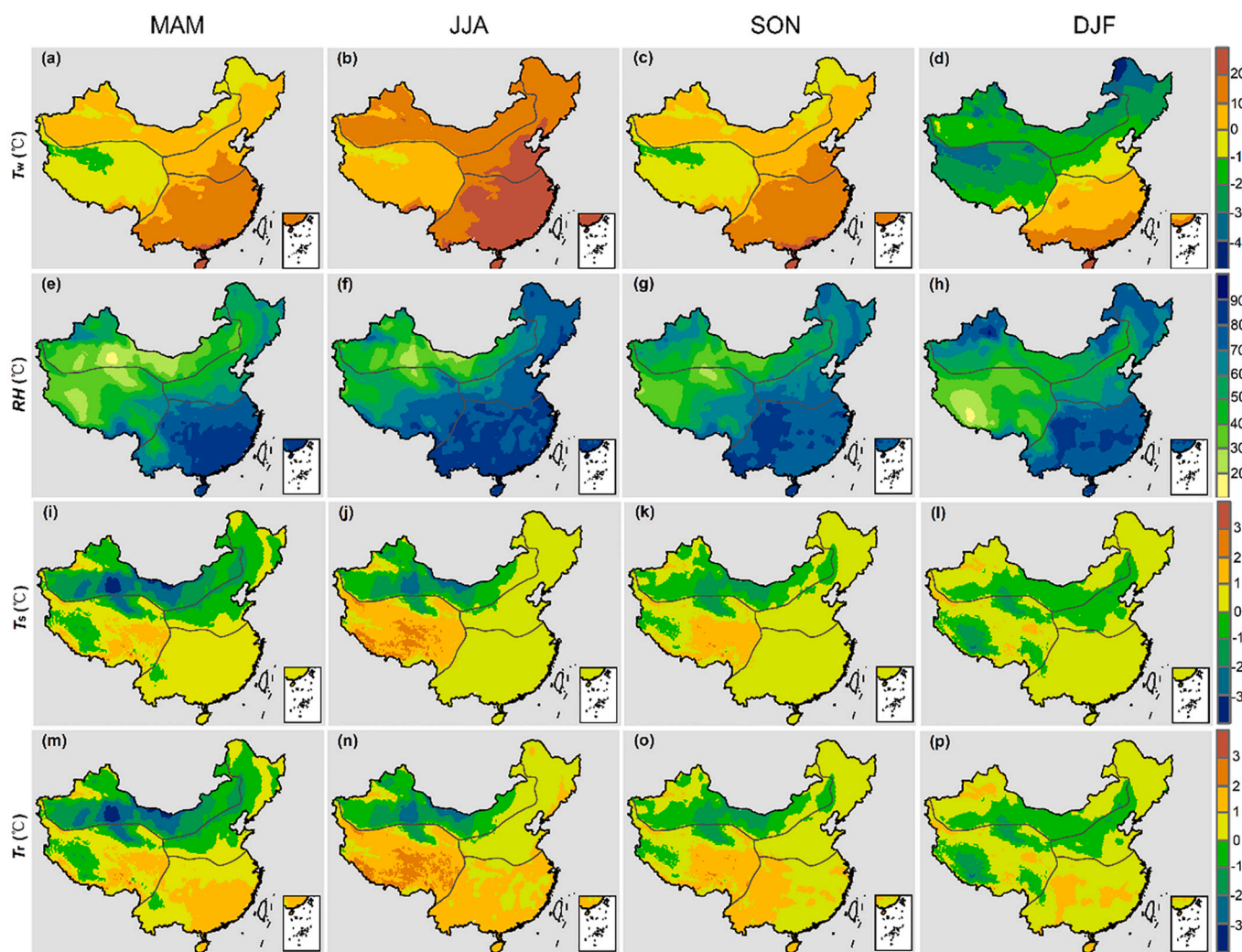


Fig. 6. Spatial distributions of the seasonal climatologies of (a–d) wet-bulb temperature ( $T_w$ ), (e–h) relative humidity ( $RH$ ), and the  $T_w$  values at which snow-sleet and sleet-rain occurred with equal frequency—that is, (i–l)  $T_s$  and (m–p)  $T_r$  during 1961–2016. Note: Spring (March–May, MAM), Summer (June–August, JJA), Autumn (September–November, SON), and Winter (December–February, DJF).

and eastern NWC, but the trends across most of the areas were not significant at the 0.05 significance level (Fig. 7(a) and Table S1). On the national scale, the annual mean precipitation significantly increased at a rate of 11.4 mm/decade across China (Fig. 8(a)). Regionally, the annual precipitation increased at rates of 2.0 mm/decade, 13.8 mm/decade, 4.3 mm/decade, and 2.8 mm/decade in NC, SC, NWC, and the TP, respectively; but the trends were not significant in NC and SC (Table S2). Seasonally, the regionally averaged precipitation increased in all four seasons across China, but the trends were only significant in winter and spring (Fig. 8(a)). The average precipitation in the TP and NC exhibited similar seasonal characteristics (Figs. 9(a–d)). However, the average precipitation in SC significantly increased in the summer and winter; while the average precipitation in NWC significantly increased in the summer, winter, and autumn (Table S2).

The annual snowfall increased significantly in northern Xinjiang and in some regions of NC, but it significantly decreased in most of the regions of the TP and in the northernmost part of NC (Fig. 7(b)). The annual mean snowfall decreased in most of the regions of SC, but this change was not significant (Fig. 7(b)). The annual mean snowfall increased in NC and NWC and decreased in SC and the TP, with rates of 1.4 mm/decade, 1.6 mm/decade,  $-0.6$  mm/decade, and  $-2.7$  mm/decade, respectively (Table S2). The different annual trends in snowfall also determined the different patterns of the snow fraction to the total precipitation. As can be seen from Fig. 10, the annual snow fraction

increased during 1961–2016 in most of the areas in NC and NWC, while it decreased in most of the TP and SC. The slopes of the annual snow fraction were 0.22%/decade,  $-0.05$ %/decade, 0.43%/decade, and  $-1.1$ %/decade in NC, SC, NWC, and the TP, respectively; but the trend was not significant in SC (Table S4). On the national scale, both the annual mean snowfall and its fraction slightly increased at rates of 1.0 mm/decade ( $P < 0.05$ ) and 0.03%/decade ( $P > 0.05$ ), respectively (Figs. 8(b) and 11(a)).

The trends of the snowfall and its fraction also varied greatly from season to season during 1961–2016 (Figs. 8(b), 9(e–h), 11(a), and 12(a–d)). Our results show that the mean snowfall decreased in summer across China, while it increased in other seasons, but the trends were only significant in autumn. The snow fraction also significantly decreased in summer, but the trends were not significant in the other seasons. Regionally, in NC, the snowfall and its fraction decreased in spring, the mean snowfall increased in both autumn and winter, but the snow fraction decreased in winter due to the large increase in the total precipitation. In NWC the snowfall increased in most of the seasons, except for summer, with the greatest increase occurring in winter (1.1%/decade). However, in contrast, the average snowfall fraction decreased in NWC during these seasons, but none of the trends were significant. On the TP, the average snowfall significantly increased in spring and winter, but it significantly decreased in summer and autumn (Table S2). However, the mean snow fraction decreased in all of the

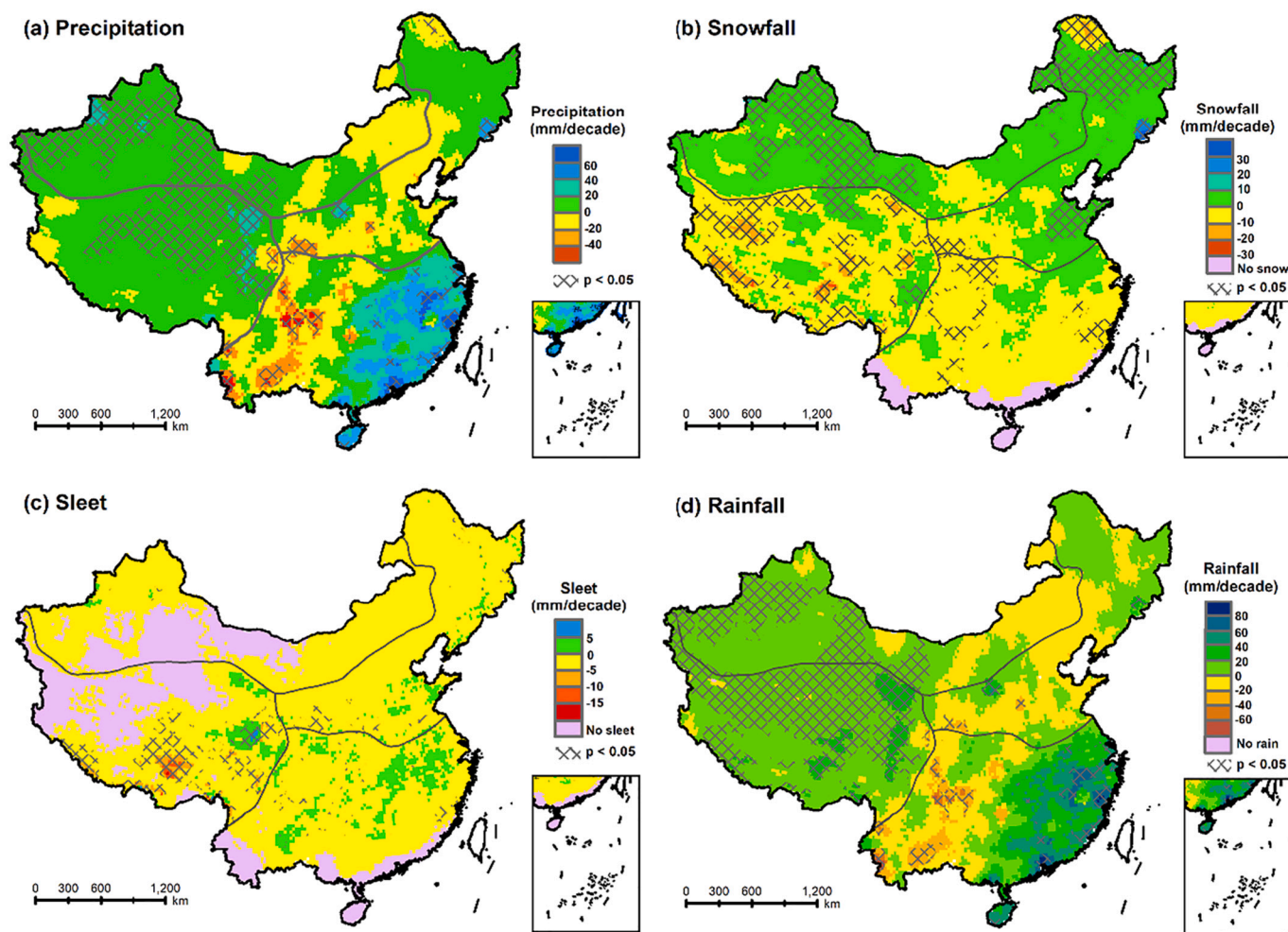


**Fig. 7.** Trends of the different forms of precipitation over China during 1961–2016: (a) total amount of precipitation, (b) snowfall, (b) sleet, and (d) rainfall. Black crosshatches in the centers of the grid cells indicate that the slope is statistically significant at the 0.05 significance level based on the nonparametric Mann–Kendall trend test.

seasons (Table S4), with the largest decreases occurring in autumn ( $-1.82\%/decade$ ), followed by summer ( $-1.61\%/decade$ ). In SC, the average snowfall decreased in all of the seasons (Table S2), and this generally decreasing trend of the snow fraction also occurred in SC (Table S4), but none of these trends were significant in any season.

The annual mean sleet decreased in all four regions (Fig. 7(c)), but the trend was only significant in the TP, with the largest decrease being  $-0.6$  mm/decade ( $P < 0.001$ ). The annual sleet fraction also significantly decreased over almost all of China, along with a decrease in sleet and a large increase in the total amount of precipitation. The rate of decreases of the annual mean sleet and its fraction across China were  $-0.3$  mm/decade and  $-0.04\%/decade$  respectively, and the large and significant decrease in the sleet and its fraction occurred in summer (Figs. 8(c) and 11(b)). Regionally, on the TP, the average sleet and its fraction significantly decreased in all of the seasons. In NC, the average sleet and its fraction exhibited a seasonal trend similar to that of the TP, but these trends were not significant. In SC, the average sleet increased in autumn and decreased in winter. In NWC, the average sleet and its fraction increased in summer and decreased in autumn, but these trends were not significant (Figs. 9(i–l) and 12(e–h), Tables S2 and S4).

During 1961–2016, the annual rainfall exhibited a pattern similar to that of the total precipitation because the rainfall accounted for the vast majority of the total precipitation (Figs. 7 and 9). The annual mean rainfall increased at rates of approximately  $0.7$  mm/decade,  $14.7$  mm/decade,  $2.9$  mm/decade,  $8.1$  mm/decade, and  $11.0$  mm/decade in NC,

SC, NWC, TP, and all of China, respectively (Fig. 8(d) and Table S2). The regionally averaged precipitation also exhibited a seasonal trend similar to that of the total precipitation in NC, SC, and NWC; but on the TP, the rainfall significantly increased in all of the seasons (Table S2). However, the annual and seasonal rain fractions exhibited a trend opposite to that of the corresponding snow fraction (Figs. 10–12). For instance, the annual rain fraction slightly decreased in most of the areas in NC and NWC, while it increased in most of the areas of the TP and SC (Fig. 10(c)).

#### 3.4. Changes in temperature thresholds ( $T_s$ and $T_r$ ) and associated $T_w$ and $RH$

Based on the parameterization scheme, the changes in the temperature thresholds ( $T_s$  and  $T_r$ ) may strongly influence the proportions of the different forms of precipitation, along with the variations in  $RH$ . As Fig. 13(b) shows, except for some regions of western NWC, most of the regions in China (approximately 71.9% of land area) exhibited decreases in the annual  $RH$  during 1961–2016, with the significant increases mainly occurring in part of SC and northeastern China (Table S5). The annual mean  $RH$  significantly decreased at rates of approximately  $-0.37\%/decade$ ,  $-0.27\%/decade$ ,  $-0.46\%/decade$ ,  $-0.39\%/decade$ , and  $-0.74\%/decade$  in all of China, NC, SC, NWC, and the TP, respectively (Table S6). Consequently, there were significant decreases in  $T_s$  and  $T_r$  across several regions in China. This may have led to more

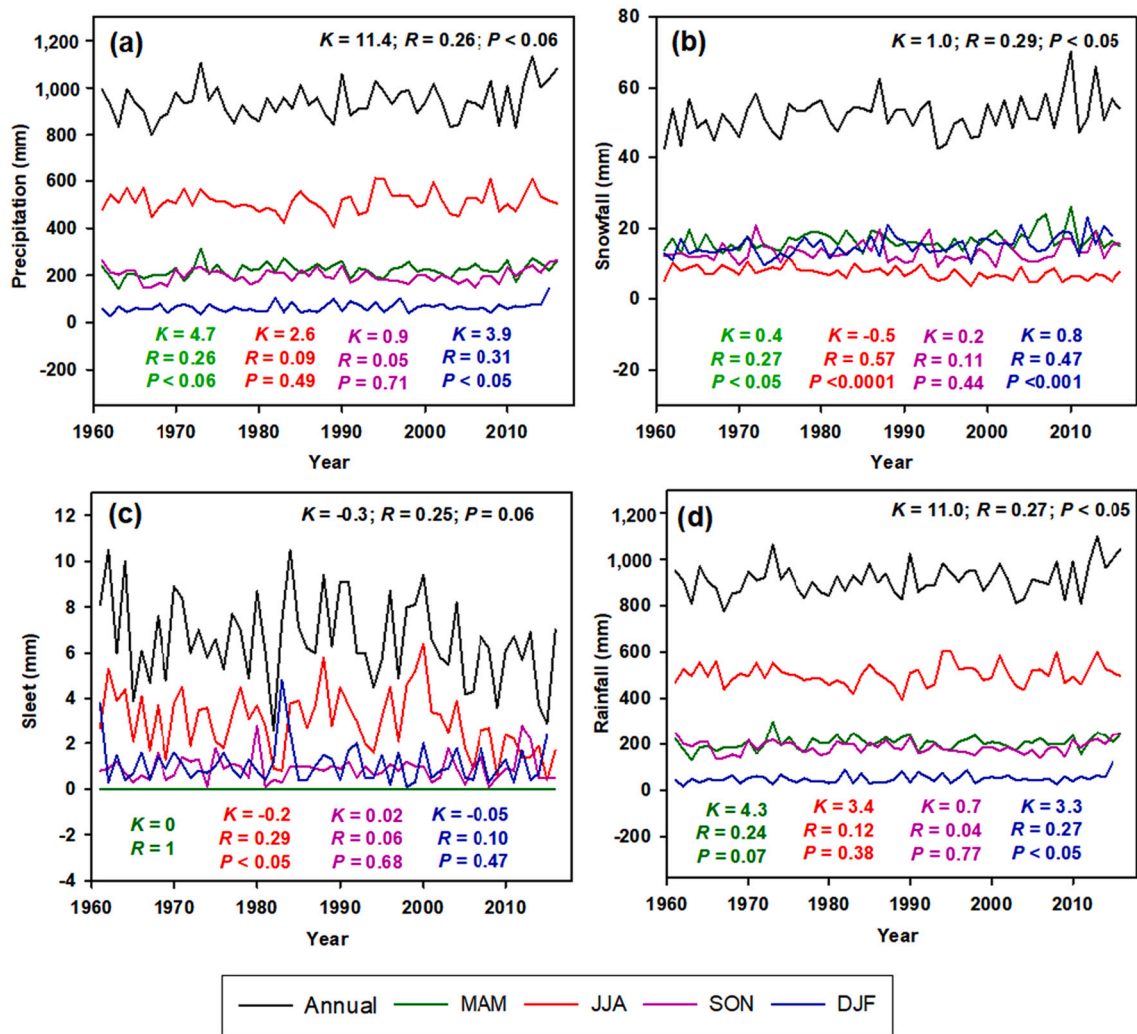


**Fig. 8.** Time series of the annual and seasonal (a) precipitation, (b) snowfall, (c) sleet, and (d) rainfall averaged over China, where  $K$ ,  $R$ , and  $P$  are the slope of the regressed line (unit: mm/decade), the regression coefficient, and the significance level, respectively. Note: Spring (March–May, MAM), Summer (June–August, JJA), Autumn (September–November, SON), and Winter (December–February, DJF).

precipitation falling as rain. The annual mean  $T_s$  and  $T_r$  decreased at rates of  $-0.006$  °C/decade and  $-0.03$  °C/decade, respectively, but there were large spatial variations (Figs. 13(c–d) and 14(c–d)). The decreasing amplitudes of the mean temperature thresholds were the largest on the TP ( $-0.07$  °C/decade, for both  $T_s$  and  $T_r$ ), followed by NWC ( $-0.04$  °C/decade for both  $T_s$  and  $T_r$ ) (Table S6).

The trends in the  $RH$  and temperature thresholds (both  $T_s$  and  $T_r$ ) also varied greatly from season to season (Fig. 15 and Tables S5–S6). The regionally averaged  $RH$  across China significantly decreased at rates of  $-0.24\%$ /decade,  $-0.46\%$ /decade,  $-0.51\%$ /decade, and  $-0.30\%$ /decade in spring, summer, autumn, and winter, respectively. However, the largest rates of the decreases occurred in spring in SC and NWC and winter in NC and the TP (Table S6). The mean  $T_r$  across China significantly decreased in all of the seasons at a rate of  $-0.03$  to  $-0.02$  °C/decade, while  $T_s$  did not exhibit a significant trend in any season (Fig. 14). Notably,  $T_s$  exhibited the largest decreases in the TP in winter and NWC in the spring ( $-0.09$  °C/decade) (Table S6).

There is no doubt that the  $T_w$  is a crucial factor affecting the form of precipitation. As Fig. 13(a) shows, the increases in  $T_w$  were very significant over almost all of China during 1961–2016. The annual mean  $T_w$  increased at a rate of  $0.21$  °C/decade across China, with the largest increase occurring in winter ( $0.44$  °C/decade) and the smallest increase occurring in summer ( $0.13$  °C/decade) (Fig. 14(a)). The annual mean  $T_w$

exhibited the largest increase on the TP and in NC (i.e.,  $0.26$  °C/decade), followed by NWC (i.e.,  $0.25$  °C/decade), and SC had the smallest rate of  $0.11$  °C/decade. Almost all of the regions experienced significant increases in all of the seasons, but the largest increases occurred in winter (Fig. 15 and Table S6). The adverse combination of the increase in  $T_w$  and the decreases in the temperature thresholds (especially  $T_r$ ) resulted in more precipitation inevitably falling as rain.

#### 4. Summary and discussion

Numerous studies have investigated the different forms of precipitation in China, especially snowfall, based on in situ observation data, temperature-based thresholds, and temperature profile methods. However, the climatology and trends of the different types of precipitation (snow, sleet, and rain) have yet to be comprehensively presented in China. In this study, the climatology and changes in the different forms of precipitation (snow, sleet, and rain) over China mainland during 1961–2016 were systematically explored using a state-of-the-art parameterization scheme and observational gridded datasets, with a maximum spatial resolution of  $0.25^\circ$ . The results show that the long-term mean annual snowfall and sleet accounted for nearly 9.6% and 0.8% of the total precipitation averaged over China, respectively. The rainfall accounted for the vast majority (89.4%) of the total

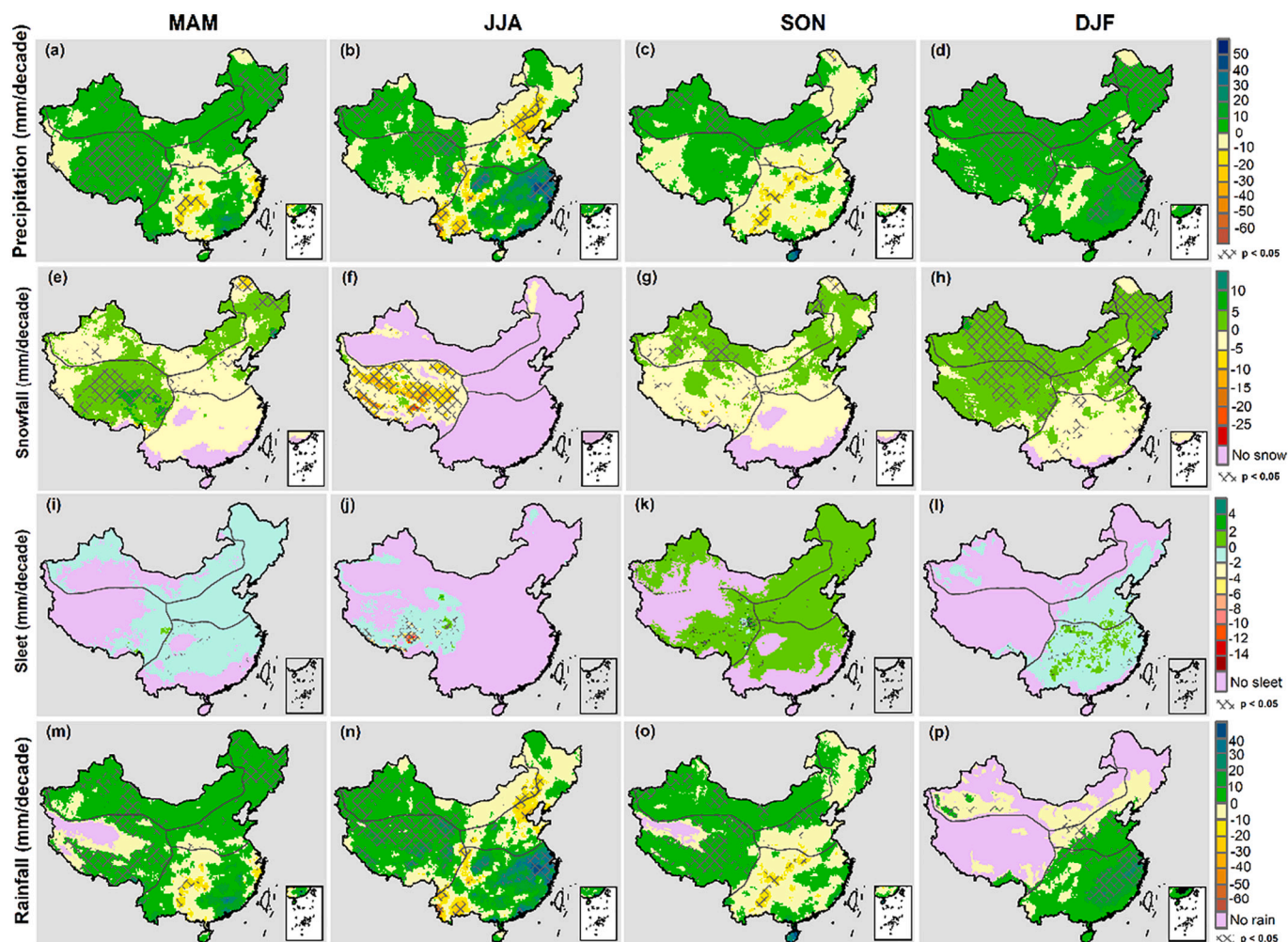


Fig. 9. Spatial distributions of the seasonal trends of the different forms of precipitation over China during 1961–2016. (a–d) total amount of precipitation, (e–h) snowfall, (i–l) sleet, and (m–p) rainfall. Note: Spring (March–May, MAM), Summer (June–August, JJA), Autumn (September–November, SON), and Winter (December–February, DJF). The black crosshatches in the centers of the grid cells indicate that the slope is statistically significant at the 0.05 significance level based on the nonparametric Mann–Kendall trend test.

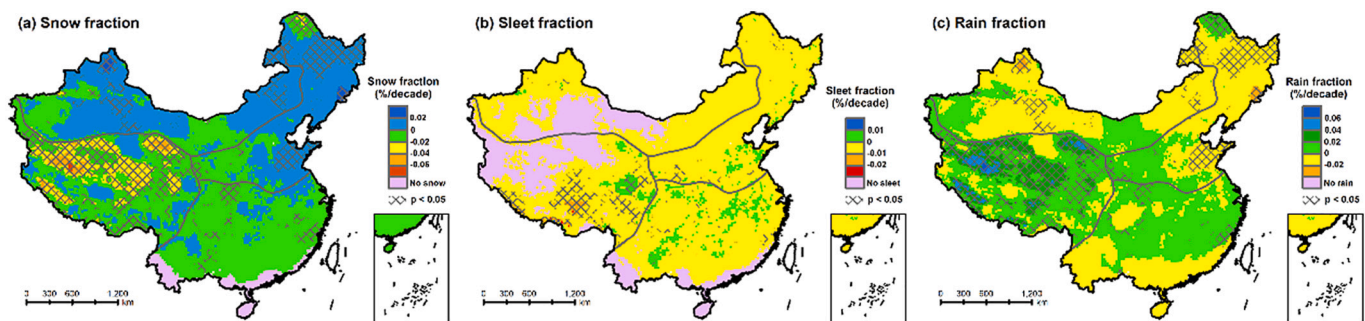


Fig. 10. Trends of the annual mean (a) snow, (b) sleet, and (c) rain fractions over China during 1961–2016. The black crosshatches indicate that the slope is statistically significant at the 0.05 significance level based on the nonparametric Mann–Kendall trend test.

precipitation, and its climatology is almost consistent with that of the total precipitation spatially. The snowfall accounted for the highest proportion of the mean annual precipitation on the TP (35.0%), with a mean annual snowfall of 142.0 mm. The sleet had high values on the southeast TP and in the middle and lower reaches of the Yangtze River Basin. From 1961 to 2016, the regionally averaged annual precipitation, rainfall, and snowfall across China significantly increased at rates of 11.4 mm/decade, 11.0 mm/decade, and 1.0 mm/decade, respectively,

whereas the annual sleet decreased at a rate of  $-0.3$  mm/decade. The annual sleet fraction also significantly decreased over almost all of China, along with a decrease in sleet and a large increase in the total precipitation. The annual mean snow (rain) fraction slightly increased (decreased) at a rate of 0.03%/decade, but the trends were not significant at the 0.05 significance level. Furthermore, the trends of the different forms of precipitation varied from region to region and from season to season. For instance, the annual snow fraction increased

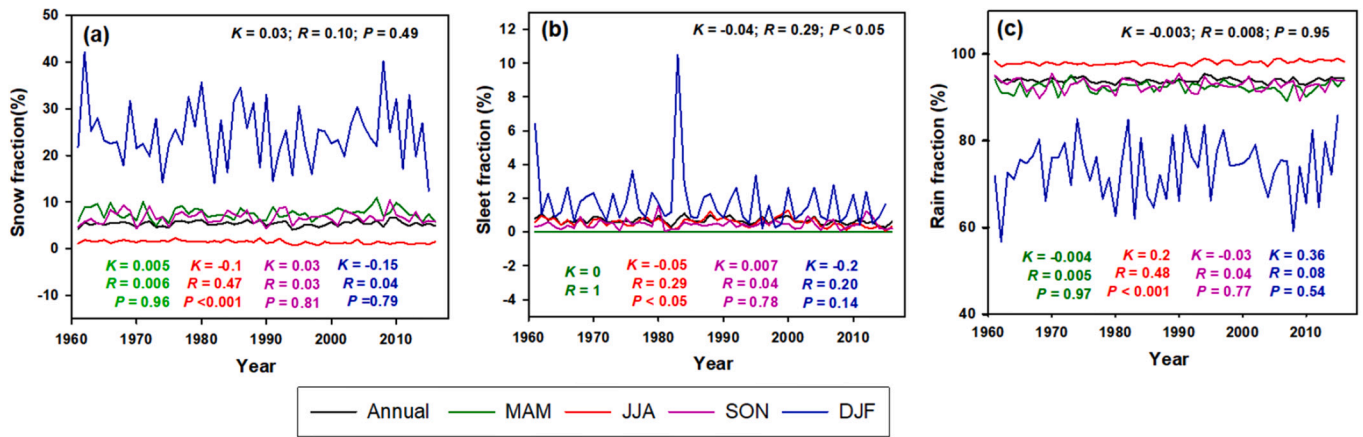


Fig. 11. Time series of the annual and seasonal (a) snow, (b) sleet, and (c) rain fractions averaged over China, where  $K$ ,  $R$ , and  $P$  are the slope of the regressed line (unit: %/decade), the regression coefficient, and the significance level, respectively. Note: Spring (March–May, MAM), Summer (June–August, JJA), Autumn (September–November, SON), and Winter (December–February, DJF).

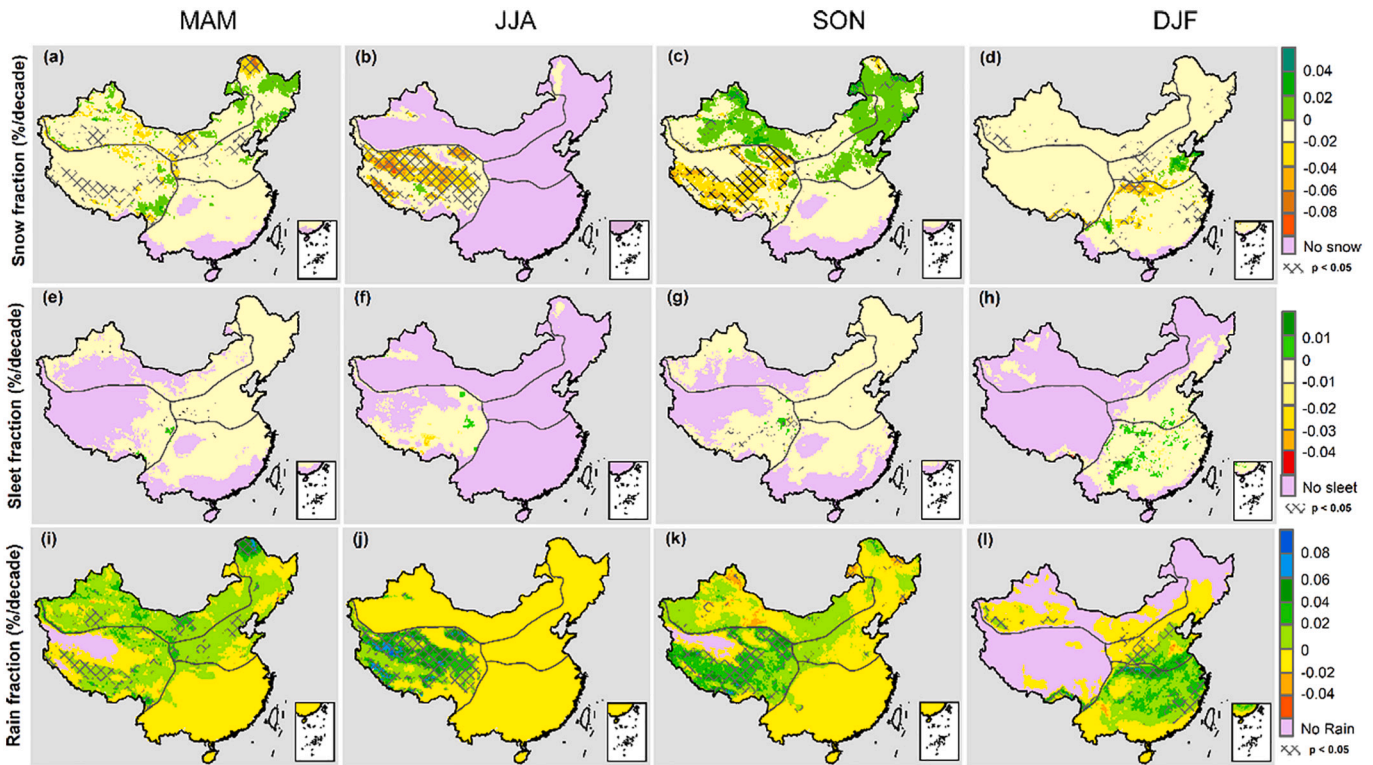
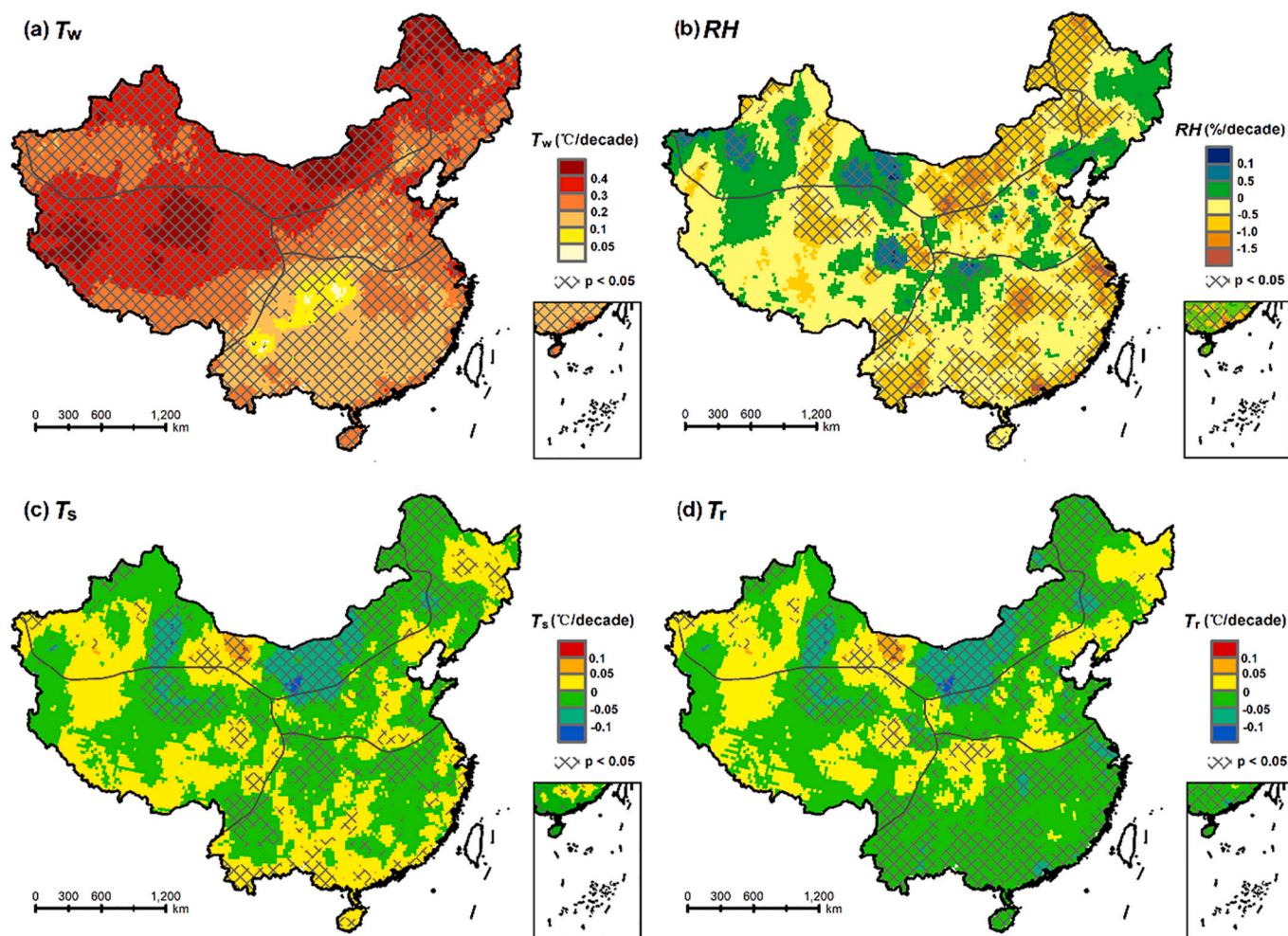


Fig. 12. Trends of the seasonal mean snow, sleet, and rain fractions over China during 1961–2016. (a–d) snow fraction, (e–h) sleet fraction, and (i–l) rain fraction. Note: Spring (March–May, MAM), Summer (June–August, JJA), Autumn (September–November, SON), and Winter (December–February, DJF). The black cross-hatches indicate that the slope is statistically significant at the 0.05 significance level based on the nonparametric Mann–Kendall trend test.

during 1961–2016 in most areas of NC and NWC, while it decreased on most of the TP and in SC, which is principally attributed to the differences in the changes in the annual snowfall in these regions.

The continuous map of the temperature thresholds over China and

their changes was further investigated for the first time and  $T_w$  and  $RH$  were analyzed. We found that the  $T_w$  at which snow and sleet (rain and sleet) occur with equal frequency, i.e.,  $T_s$  ( $T_r$ ), varies significantly across China due to the heterogeneous  $RH$  and complex topography. The



**Fig. 13.** Trends of (a) wet-bulb temperature ( $T_w$ ), (b) relative humidity ( $RH$ ), and the  $T_w$  values at which snow-sleet and sleet-rain occurred with equal frequency—that is, (c)  $T_s$  and (d)  $T_r$  during 1961–2016. The black crosshatches in the centers of the grid cells indicate that the slope is statistically significant at the 0.05 significance level based on the nonparametric Mann–Kendall trend test.

climatology of  $RH$  is spatially consistent with that of the total precipitation. The regionally averaged mean  $T_s$  ( $T_r$ ) is 0.1 °C (0.3 °C) in China, with the highest values of both  $T_s$  and  $T_r$  occurring on the southeast TP, and the lowest values occurring in the desert areas of NWC. Most regions experienced significant decreases in the temperature thresholds (especially for  $T_r$ ) with decreasing  $RH$ . The regionally averaged annual  $RH$  and  $T_r$  significantly decreased at rates of approximately  $-0.37\%/decade$  and  $-0.03\text{ °C}/decade$ , respectively. Almost all of the regions experienced significant increases in  $T_w$ , especially on the TP and during the winter and spring.

Overall, the estimated climatologies and trends of the snowfall and its fraction in China are consistent with those reported in previous regional studies based on observation data (Zhao et al., 2009; Liu et al., 2012; Guo and Li, 2015; Li et al., 2022), and air temperature-based thresholds (Wang et al., 2016; Wang et al., 2017a; Wang et al., 2017b; Hou et al., 2019; Li et al., 2022). The estimated spatiotemporal patterns of snowfall across China were also in line with those in previous studies on snow cover and snow depth at both the national and regional scales

(e.g., Wang et al., 2017b; Ma et al., 2020; You et al., 2020). These can be considered to be an indirect verification of the parameterization scheme used in this study. The uncertainty sources of estimated different forms of precipitation mainly include the parameterization scheme and daily weather data as input (including air temperature, precipitation,  $RH$ , and surface pressure). The parameterization scheme can be considered as state-of-the-art with three main advantages in this study: (a) the scheme was based on all known environmental variables that affect precipitation in a physical sense, including wet-bulb temperature, relative humidity, surface pressure, and elevation information; (b) it reflects spatial difference in the temperature threshold for discriminating between precipitation types; and (c) it was developed based on weather station data in China. In contrast, other methods are often derived from regional vertical profiles of air temperature and other atmospheric conditions or simple relationships between the existing observed precipitation types and the air temperature. Furthermore, the temperature thresholds are commonly spatially and temporally uniform, i.e., the spatiotemporal heterogeneity of the temperature thresholds was ignored in these

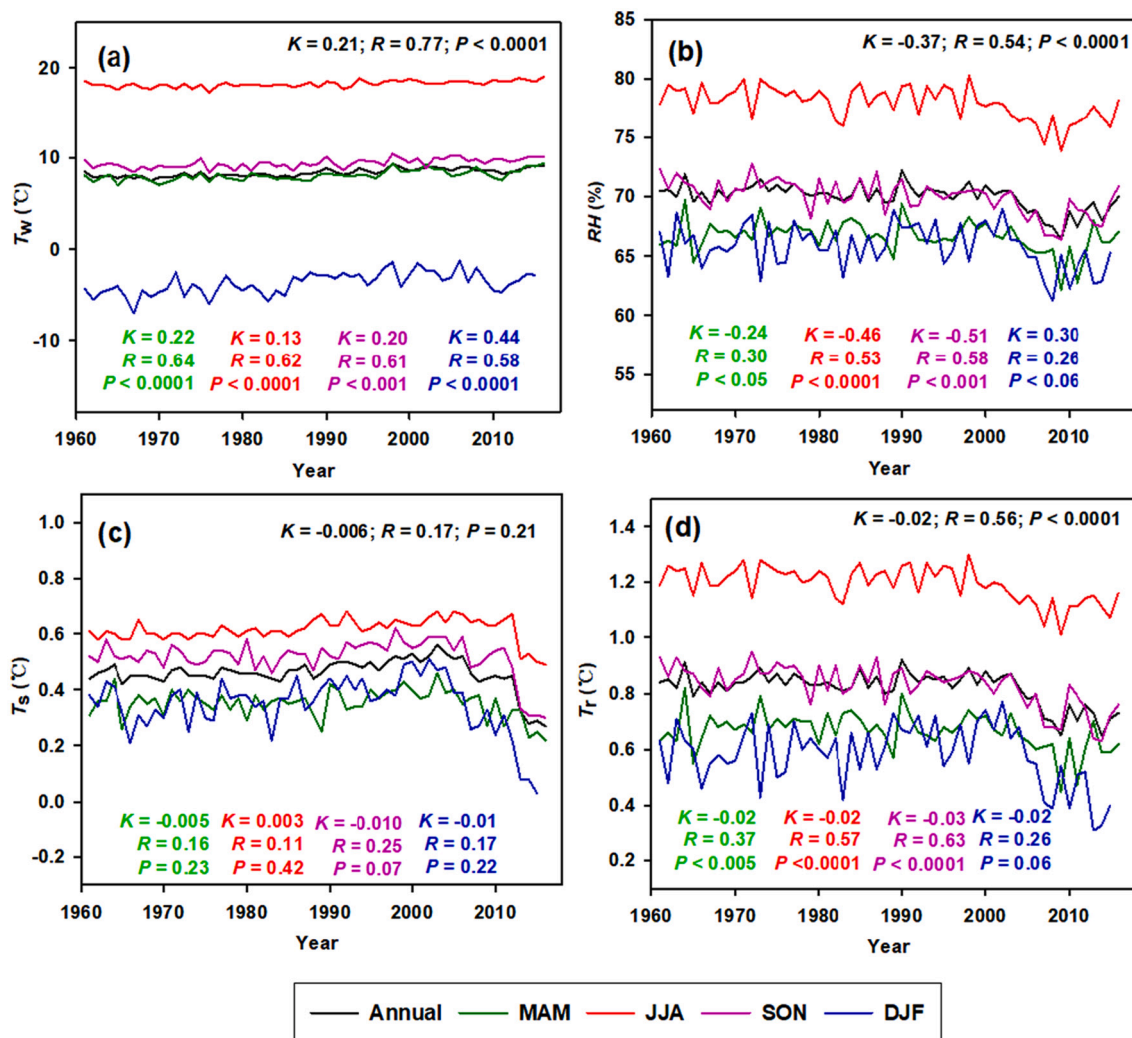


**Fig. 14.** Time series of the annual and seasonal (a) wet-bulb temperature ( $T_w$ ), (b) relative humidity ( $RH$ ), and the  $T_w$  values at which snow-sleet and sleet-rain occurred with equal frequency—that is, (c)  $T_s$  and (d)  $T_r$  averaged over China, where  $K$ ,  $R$ , and  $P$  are the slope of the regressed line (unit:  $^{\circ}C/decade$  for  $T_s$ ,  $T_r$ , and  $T_w$ , and  $\%/decade$  for  $RH$ ), the regression coefficient, and the significance level, respectively. Note: Spring (March–May, MAM), Summer (June–August, JJA), Autumn (September–November, SON), and Winter (December–February, DJF).

schemes. [Ding et al. \(2014\)](#) evaluated and concluded that the scheme had better accuracy than most schemes used in hydrological and land surface models at present. Regarding the uncertainty of input data, the error in western China is unavoidably large, especially for the alpine regions such as northern TP, due to complex terrain and the scarcity of site observations. Nevertheless, we selected the observational CN05.1 gridded dataset as the main input of the parameterization scheme, which was interpolated based on 2416 stations in China ([Wu and Gao, 2013](#)). To our knowledge, it can be considered the most reliable gridded data for the study region. In addition, the parameterization scheme proposed by [Ding et al. \(2014\)](#) was based on ground-based observation. To verify if the site-based scheme can be applied to work at the grid-scale well, we conducted a comparison between our results and the those in previous studies based on the same scheme but site-scale data, and found that they are essentially in agreement, such as in the TP ([Deng et al., 2017](#)), Tianshan Mountains ([Li et al., 2020](#)), northern Xinjiang

([Yang et al., 2020](#)), and overall China ([Zhang et al., 2016a](#)).

Our results also demonstrated that the adverse combination of the increase in  $T_w$  and the decreases in the temperature thresholds inevitably resulted in more precipitation falling as rain in China. However, their relative contributions still need to be quantified. In addition, more attention should also be paid to the spatiotemporal heterogeneity of the temperature thresholds when discriminating precipitation types in the future.

**CRediT authorship contribution statement**

**Bo Su:** Conceptualization, Visualization, Writing – original draft, Writing – review & editing, Funding acquisition. **Cunde Xiao:** Conceptualization, Writing – review & editing, Funding acquisition, Supervision. **Hongyu Zhao:** Writing – review & editing. **Yi Huang:** Writing – review & editing. **Tingfeng Dou:** Conceptualization, Writing –

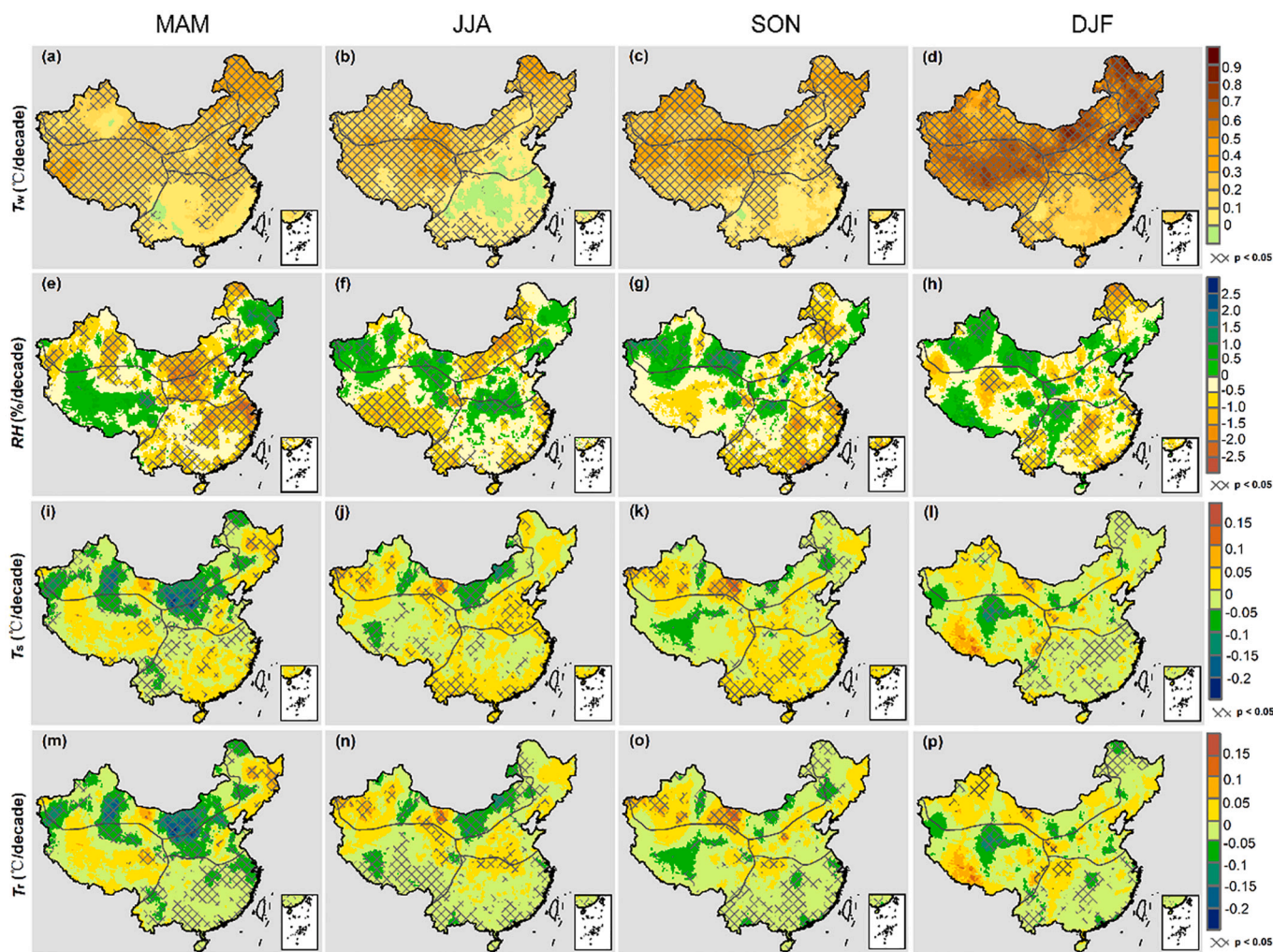


**Fig. 15.** Trends of (a–d) wet-bulb temperature ( $T_w$ ), (e–h) relative humidity ( $RH$ ), and the  $T_w$  values at which snow-sleet and sleet-rain occurred with equal frequency—that is, (i–l)  $T_s$  and (m–p)  $T_r$  during 1961–2016. Note: Spring (March–May, MAM), Summer (June–August, JJA), Autumn (September–November, SON), and Winter (December–February, DJF). The black crosshatches in the centers of the grid cell indicate that the slope is statistically significant at the 0.05 significance level based on the nonparametric Mann–Kendall trend test.

review & editing. **Xuejia Wang:** Conceptualization, Writing – review & editing. **Deliang Chen:** Conceptualization, Writing – review & editing, Funding acquisition, Supervision.

**Declaration of Competing Interest**

The authors declare that they have no conflict of interest.

**Acknowledgements**

This research was jointly funded by the National Natural Science Foundation of China (NSFC grant Nos. 41690145) and the Strategic Priority Research Program of the Chinese Academy of Sciences (Grant No. XDA20060401), and National Foundation of China Scholarship Council (Grant No. 201906040104).

**Appendix A. Supplementary data**

Supplementary data to this article can be found online at <https://doi.org/10.1016/j.atmosres.2022.106078>.

**References**

Berghuijs, W.R., Woods, M. Hrachowitz, 2014. A precipitation shift from snow towards rain leads to a decrease in streamflow. *Nature. Climate Change* 4 (7), 583–586.

Chen, Y., Li, W., Deng, H., et al., 2016. Changes in Central Asia’s water tower: past, present and future. *Sci. Rep.* 6 (1), 1–12.

Deng, H., Pepin, N.C., Chen, Y., 2017. Changes of snowfall under warming in the Tibetan Plateau. *Journal of Geophysical Research: Atmospheres* 122 (14), 7323–7341.

Deng, K., Jiang, X., Hu, C., et al., 2020. More frequent summer heat waves in southwestern China linked to the recent declining of Arctic Sea ice. *Environ. Res. Lett.* 15 (7), 074011.

Ding, Y., 2013. *Climate in China*. Science Press, Beijing (In Chinese with English abstract).

Ding, B., Yang, K., Qin, J., et al., 2014. The dependence of precipitation types on surface elevation and meteorological conditions and its parameterization. *J. Hydrol.* 513, 154–163.

Ding, B., Yang, K., Yang, W., et al., 2017. Development of a Water and Enthalpy Budget-based Glacier mass balance Model (WEB-GM) and its preliminary validation. *Water Resour. Res.* 53 (4), 3146–3178.

Dou, T., Xiao, C., Liu, J., et al., 2021. Trends and spatial variation in rain-on-snow events over the Arctic Ocean during the early melt season. *Cryosphere* 15 (2), 883–895.

Flanner, M.G., Shell, K.M., Barlage, M., et al., 2011. Radiative forcing and albedo feedback from the Northern Hemisphere cryosphere between 1979 and 2008. *Nat. Geosci.* 4 (3), 151–155.

Guo, L., Li, L., 2015. Variation of the proportion of precipitation occurring as snow in the Tian Shan Mountains, China. *International Journal of Climatology* 35 (7), 1379–1393.

Guo, D., Sun, J., Yu, E., 2018. Evaluation of CORDEX regional climate models in simulating temperature and precipitation over the Tibetan Plateau. *Atmospheric and Oceanic Science Letters* 11 (3), 219–227.

- Han, W., Xiao, C., Dou, T., et al., 2018. Arctic has been going through a transition from solid precipitation to liquid precipitation in spring (in Chinese). *Chin. Sci. Bull.* 63, 1154–1162.
- Hou, B., Jiang, C., Sun, J., 2019. Analysis of Precipitation Forms Characteristics in Heilongjiang Province based on Snowfall/Precipitation Ratio. *Plateau Meteorology* 38, 781–793 (In Chinese with English abstract).
- Huntington, T.G., Hodgkins, G.A., Keim, B.D., et al., 2004. Changes in the proportion of precipitation occurring as snow in New England (1949–2000). *J. Clim.* 17 (13), 2626–2636.
- IPCC, 2021. *Climate Change 2021: The Physical Science Basis. Contribution of Working Group I to 962 the Six Assessment Report of the Intergovernmental Panel on Climate Change.* Cambridge, United 963 Kingdom and. Cambridge University Press, New York, NY, USA.
- Irannezhad, M., Ronkanen, A.K., Kiani, S., et al., 2017. Long-term variability and trends in annual snowfall/total precipitation ratio in Finland and the role of atmospheric circulation patterns. *Cold Reg. Sci. Technol.* 143, 23–31.
- Jennings, K.S., Winchell, T.S., Livneh, B., et al., 2018. Spatial variation of the rain–snow temperature threshold across the Northern Hemisphere. *Nat. Commun.* 9 (1), 1–9.
- Jiang, C., Sun, J., 2019. Analysis of precipitation forms characteristics in Heilongjiang province based on snowfall/precipitation ratio. *Plateau Meteorol.* 38 (4), 781–793 (in Chinese with English abstract).
- Kendall, M.G., 1948. *Rank Correlation Methods.* Griffin, London.
- Knowles, N., Dettinger, M.D., Cayan, D.R., 2006. Trends in snowfall versus rainfall in the western United States. *J. Clim.* 19 (18), 4545–4559.
- Krasting, J.P., Broccoli, A.J., Dixon, K.W., et al., 2013. Future changes in Northern Hemisphere snowfall. *J. Clim.* 26 (20), 7813–7828.
- Li, Z., Chen, Y., Li, Y., et al., 2020. Declining snowfall fraction in the alpine regions, Central Asia. *Scientific reports* 10 (1), 1–12.
- Li, D., Qi, Y., Chen, D., 2022. Changes in rain and snow over the Tibetan Plateau based on IMERG and Ground-based observation. *J. Hydrol.* 606. <https://doi.org/10.1016/j.jhydrol.2021.127400>.
- Liu, Y., Ren, G., Yu, H., 2012. Climatology of Snow in China. *Sci. Geogr. Sin.* 32 (10), 1176–1185 (in Chinese with English abstract).
- Loth, B., Graf, H.F., Oberhuber, J.M., 1993. Snow cover model for global climate simulations. *Journal of Geophysical Research: Atmospheres* 98 (D6), 10451–10464.
- Ma, N., Yu, K., Zhang, Y., et al., 2020. Ground observed climatology and trend in snow cover phenology across China with consideration of snow-free breaks. *Clim. Dyn.* 55 (9), 2867–2887.
- Mankin, J.S., Diffenbaugh, N.S., 2015. Influence of temperature and precipitation variability on near-term snow trends. *Clim. Dyn.* 45 (3), 1099–1116.
- Mann, H.B., 1945. Nonparametric Tests against Trend. *Econometrica* 13, 245–259.
- Marks, D., Dozier, J., Davis, R.E., 1992. Climate and energy exchange at the snow surface in the alpine region of the Sierra Nevada: 1. Meteorological measurements and monitoring. *Water Resour. Res.* 28 (11), 3029–3042.
- Murray, F.W., 1967. On the computation of saturation vapor pressure. *J. Appl. Meteorol.* 6 (1), 203–204.
- Musselman, K.N., Addor, N., Vano, J.A., et al., 2021. Winter melt trends portend widespread declines in snow water resources. *Nat. Clim. Chang.* 11 (5), 418–424.
- Räisänen, J., 2008. Warmer climate: less or more snow? *Clim. Dyn.* 30 (2), 307–319.
- Sen, P.K., 1968. Estimates of the Regression Coefficient based on Kendall's Tau. *J. Am. Stat. Assoc.* 63, 1379–1389.
- Serquet, G., Marty, C., Dulex, J., et al., 2011. Seasonal trends and temperature dependence of the snowfall/precipitation-day ratio in Switzerland. *Geophys. Res. Lett.* 38 (7).
- Song, F., Qi, H., 2007. Changes in winter snowfall/precipitation ratio in the contiguous United States. *Journal of Geophysical Research: Atmospheres* 112 (D15).
- Su, B., Xiao, C., Chen, D., et al., 2022. Glacier change in China over past decades: spatiotemporal patterns and influencing factors. *Earth Sci. Rev.* 226, 103926 <https://doi.org/10.1016/j.earscirev.2022.103926>.
- Wang, J., Zhang, M., Wang, S., et al., 2016. Change of snowfall/rainfall ratio in the Tibetan Plateau based on a gridded dataset with high resolution during 1961–2013. *Acta Geograph. Sin.* 71 (1), 142–152 (in Chinese with English abstract).
- Wang, J., Zhang, M., Wang, S., et al., 2017a. Change of Snowfall/Rainfall Ratio in Xinjiang during the Period of 1961–2013. *Arid Zone Research* 34 (4). <https://doi.org/10.13866/j.azr.2017.04.23> (in Chinese with English abstract).
- Wang, Z., Wu, R., Hang, G., 2017b. Low-frequency snow changes over the Tibetan Plateau. *Int. J. Climatol.* <https://doi.org/10.1002/joc.5221>.
- Wang, X., Chen, D., Pang, G., et al., 2020. A climatology of surface–air temperature difference over the Tibetan Plateau: results from multi-source reanalyses. *Int. J. Climatol.* 40 (14), 6080–6094.
- Wu, J., Gao, X.J., 2013. A gridded daily observation dataset over China region and comparison with the other datasets. *Chin. J. Geophys.* 56 (4), 1102–1111 (in Chinese with English abstract).
- Yang, T., Li, Q., Liu, W., et al., 2020. Spatiotemporal variability of snowfall and its concentration in northern Xinjiang, Northwest China. *Theoretical and Applied Climatology* 139 (3), 1247–1259.
- Yang, D., Ding, M., Dou, T., et al., 2021. On the differences in Precipitation Type between the Arctic, Antarctica and Tibetan Plateau. *Front. Earth Sci.* 9, 19.
- Yao, T., Thompson, L., Yang, W., et al., 2012. Different glacier status with atmospheric circulations in Tibetan Plateau and surroundings. *Nat. Clim. Chang.* 2 (9), 663–667.
- Ye, H., Cohen, J., Rawlins, M., 2013. Discrimination of Solid from Liquid Precipitation over Northern Eurasia using Surface Atmospheric Conditions. *J. Hydrometeorol.* 14 (4), 1345–1355.
- You, Q., Wu, T., Shen, L., et al., 2020. Review of snow cover variation over the Tibetan Plateau and its influence on the broad climate system. *Earth Sci. Rev.* 201, 103043.
- Zhang, D., Cong, Z., Ni, G., 2016a. Snowfall changes in China during 1956–2010. *Journal of Tsinghua University (Sci&Technol)* 56 (4), 381–386 (In Chinese with English abstract).
- Zhang, R., Zhang, R., Zuo, Z., 2016b. An Overview of Wintertime Snow Cover Characteristics over China and the Impact of Eurasian Snow Cover on Chinese climate. *Journal of Applied Meteorological Science* 27 (5), 513–526 (In Chinese with English abstract).
- Zhang, G., Yao, T., Xie, H., et al., 2020. Response of Tibetan Plateau's lakes to climate changes: trend, pattern, and mechanisms. *Earth Sci. Rev.* 103269.
- Zhao, J., 2005. *Chinese Physical Geography.* High Education Press, Beijing.
- Zhao, C., Wang, J., Yan, X., et al., 2009. Climatic characteristics and regionalization of winter snowfall in Northeast China. *Journal of Natural Disasters* 18 (5), 29–35 (In Chinese with English abstract).
- Zhong, X., Zhang, T., Kang, S., et al., 2018. Spatiotemporal variability of snow depth across the Eurasian continent from 1966 to 2012. *Cryosphere* 12 (1), 227–245.